Heliyon 8 (2022) e10778

Contents lists available at ScienceDirect

Heliyon

journal homepage: www.cell.com/heliyon

Research article

Accurate *in vivo* real-time determination of the hydrogen concentration in different tissues of mice after hydrogen inhalation

Wenjun Zhu [a,b,1], Qianqian Gu [a,1], Boyan Liu [a], Yanhong Si [a], Huirong Sun [a,b], Jingjie Zhong [a,b], Yi Lu [a,b], Dan Wang [a,b], Junli Xue [a,*], Shucun Qin [a,**]

[a] *Taishan Institute for Hydrogen Biomedicine, School of Basic Medical Sciences, The Second Affiliated Hospital of Shandong First Medical University & Shandong Academy of Medical Sciences, Tai'an, Shandong Province, China*

[b] *School of Public Health, Shandong First Medical University & Shandong Academy of Medical Sciences, Tai'an, Shandong Province, China*

ARTICLE INFO

Keywords:
Hydrogen concentration
Real-time monitoring
Various tissues
Electrochemical sensor
In vivo
Mice

ABSTRACT

As an antioxidant, anti-inflammatory and anti-apoptotic agent, hydrogen (H_2) shows a promising potential in basic and clinical research against various diseases owing to its safety and efficacy. However, knowledge involving its underlying mechanisms of action, dosage effects, and dose duration remains limited. Previously, the dynamics of H_2 concentrations in different tissues of rats after exogenous H_2 inhalation had been detected by our team. Here, sequential changes of H_2 concentrations in different tissues of another most commonly used experimental rodent mice were monitored in real time with an electrochemical H_2 gas sensor during continuous different concentrations of H_2 inhalation targeting on five tissues including brain, liver, spleen, kidney, and gastrocnemius. The results showed that the H_2 saturation concentrations varied among tissues significantly regardless of the concentration of H_2 inhaled, and they were detected the highest in the kidney but the lowest in the gastrocnemius. Meantime, it required a significant longer time to saturate in the thigh muscle. By comparing the H_2 saturation concentrations of mice and rats, we found that there were no differences detected in most tissues except the kidney and spleen. Both gas diffusion and bloodstream transport could help the H_2 reach to most organs. The results provide data reference for dosage selection, dose duration determination to ensure optimal therapeutic effects of H_2 for mice experiments.

1. Introduction

As the number one element in the periodic table, hydrogen has the simplest structure and the smallest molecular weight. It usually forms a diatomic molecule (H_2) with a low density and physical non-polarity, which enables it to disperse quickly and even penetrate the organelle membrane. Although H_2 is an inert gas, its role in the prevention and treatment of various diseases has created quite a stir since 2007, when Ohsawa's team reported its antioxidant effect in a rodent model of ischemia-reperfusion injury (Ohsawa et al., 2007). Given its safety and effectiveness, H_2 is always commanding attention with numerous animal studies and clinical trials. Many countries and regions including USA, Japan, Europe, and China have recognized H_2 as a food additive, despite it is not accepted globally (Liu et al., 2022). It is worth mentioning that H_2 has played an indelible role in the treatment of the latest outbreak of coronavirus disease 2019 (COVID-19) (Guan et al., 2020).

It must be said that hydrogen biomedicine has indeed mushroomed in recent decades, but two major problems are also hindering its further development. One is the undefined mechanism. Currently, the protective effects of H_2 are largely attributed to its antioxidant, anti-inflammatory, and anti-apoptotic properties (Liu et al., 2021; Russell et al., 2021). Although few reports have proposed the effects on bio-enzyme activity, protein structural properties, and gut microbiota/short-chain fatty acids axis (Cheng et al., 2020; Ma et al., 2020; Ge et al., 2022), yet the direct target is still being unidentified. The other is the undetermined dose-effect, which is seriously affected by the diffusivity of H_2 and the instability of H_2 donor. At present, exogenous H_2 can be ingested by organisms via various methods mainly including H_2-rich water drinking, H_2-rich saline injection and H_2 inhalation (Ge et al., 2017). In the

* Corresponding author.
** Corresponding author.
E-mail addresses: xuejunli1988@126.com (J. Xue), scqin@sdfmu.edu.cn (S. Qin).
[1] These authors contributed equally to this work.

https://doi.org/10.1016/j.heliyon.2022.e10778
Received 27 February 2022; Received in revised form 11 May 2022; Accepted 22 September 2022

processes of different administrations, the H_2 saturation concentration and the saturation rates in various tissues are considered as important reference for the optimal administration selection. As the most straightforward therapeutic method, H_2 inhalation has been widely used since the first sensational report in 2007 (Ohsawa et al., 2007). Several previous studies have reported changes of H_2 concentrations in tissues of rats after exogenous H_2 inhalation (Liu et al., 2014; Yamamoto et al., 2019). However, greater inaccuracy tends to occur in results of *ex vivo* detection attributed to the rapid diffusion of H_2 in tissues during samples processing even by the aid of glass containers (Liu et al., 2014). In addition, only single concentration of H_2 (3%) was inhaled and the H_2 distribution in different tissues may differ during and after other concentrations of H_2 administration (Yamamoto et al., 2019). Recently, our team monitored the real-time H_2 concentrations in various tissues of rats during three doses of exogenous H_2 (4%, 42%, 67%; *v/v*) were inhaled. In particular, the electrochemical H_2 sensor was adopted creatively during the experiments and the dose-dependent response was revealed for the first time (Liu et al., 2022).

Since both mice and rats are the most commonly used experimental rodents in basic research, we further measured the sequential changes of H_2 concentrations over time in different tissues after mice inhaled different concentrations of exogenous H_2. Considering both the easy collection and blood flow of the tissues, five tissues including brain, liver, spleen, kidney, and gastrocnemius with relatively large blood flow were targeted here. We hoped that the results could provide fundamental data reference for dose-effect studies and the determination of H_2 inhalation duration in mouse experiments to ensure the optimum effects of H_2.

2. Materials and methods

2.1. Preparation of exogenous H_2

Here, mice inhaled three different concentrations of exogenous H_2 (4%, 42%, 67%; *v/v*) using our self-made device (Liu et al., 2022). The H_2 concentration of the mixed gas was determined using a H_2 detector (XP-3140, New Cosmos Electric Co., Ltd., Osaka, Japan). 4% H_2 was used in the sensational article published by Japanese scholars in 2007 (Ohsawa et al., 2007), and then the protective role of low concentration of H_2 was reported in many diseases. Meanwhile, commercial machines produced 67% H_2 have been applied widely in clinical practice. 42% H_2 was selected as the intermediate concentration based on literature review (Huang et al., 2019). So here, these three concentrations of H_2 were used, which covered low, medium, and high concentrations.

2.2. Operation in animal experiments

25 eight-week-old SPF-level C57BL/6J mice weighing about 20 g were purchased from Jinan Pengyue Experimental Animal Breeding Co., Ltd., Shandong Province, China. All mice were housed under standard conditions (22 ± 1 °C; 12/12 h light/dark cycle) with water and food *ad libitum* for at least one-week acclimatization. Then the mice were anesthetized by an intraperitoneal injection of 20% urethane (1.4 g/kg of bodyweight, Shanghai Aladdin Biochemical Technology Co., Ltd., China). Complete anesthesia was confirmed by muscle relaxation, disappearance of the corneal reflex and smooth breathing of mice. Then, the animals were dissected on a heating plate with constant temperature of 38 °C and then tissues to be measured were exposed. To minimize the damage to the mice and create a more realistic simulation of the *in-vivo* condition, the operative incision should be made as small as possible. After the mice were secured, tip of the microelectrode was then dipped into the exposed tissue. Here, five representative tissues including the brain, median lobe of the liver, spleen, kidney, and rear gastrocnemius muscle, were targeted (Figure 1). All animal procedures were conducted following the guidelines of the laboratory animal ethics committee of Shandong First Medical University and Shandong Academy of Medical Sciences.

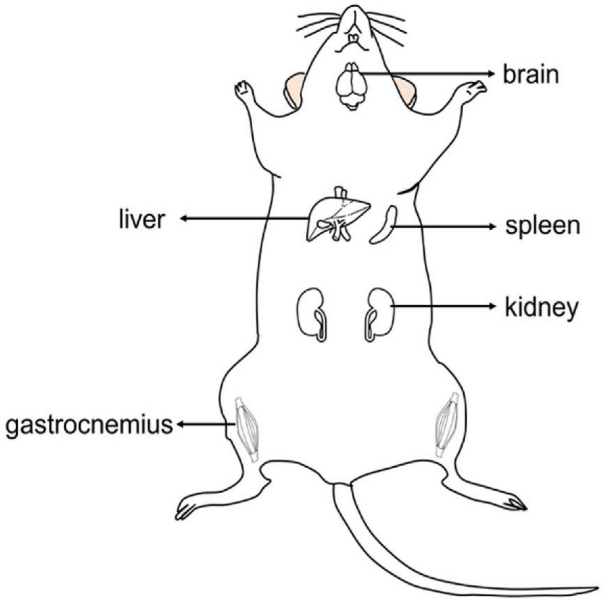

Figure 1. Five representative tissues of mice targeted for H_2 concentration measurements.

2.3. H_2 concentration measurement by electrochemical H_2 sensor

An electrochemical H_2 sensor (40–60 μm tip diameter) assembled on a micromanipulator and connected to a multimeter (Unisense, Aarhus, Denmark) was used to monitor the H_2 concentrations of different tissues. Before experiments, the H_2 sensor was calibrated, and a standard curve was established by diluting the H_2-saturated phosphate-buffered saline at 38 °C. For *in vivo* measurements, the needle sensor tip was placed less than 1 mm into the exposed tissue. Initially, a stable baseline was obtained by supplying only air. Then, the mice were continuously supplied with the required concentration of H_2 until the H_2 concentration in the measured tissue reached the plateau stage. After that, pure air was supplied and the decline curve of H_2 concentration was recorded until it returned to the baseline level again. At least three independent measurements were conducted for each tissue ($n \geq 3$). The H_2 sensor was rinsed with 0.01M hydrochloric acid between animals to remove the substances on the sensor tip.

2.4. Statistical analysis

Data are expressed as the mean ± SD (standard deviation). One-way analysis of variance followed by least significant difference (LSD) *post hoc* test was used for the data conforming to normal distribution to compare the H_2 concentrations between multi-measurement sites. Otherwise, Kruskal-Wallis multiple tests were performed. The *independent samples t-test* was used for comparison between the two groups. The $P < 0.05$ was considered significant. All data were analyzed using SPSS version 26.0 (IBM, Armonk, NY, USA) and graphed using GraphPad Prism 8.0.1 (GraphPad Software Inc., La Jolla, CA).

3. Results

3.1. Real-time curve of H_2 concentration in different tissues

The real-time concentrations of H_2 in five different tissues of mice after different concentrations of exogenous H_2 inhalation were displayed in Figures 2A–C. It could be seen that the H_2 concentrations in five tissues of mice increased significantly over time during the H_2 inhalation of any concentration. However, the rising rate and amplitude

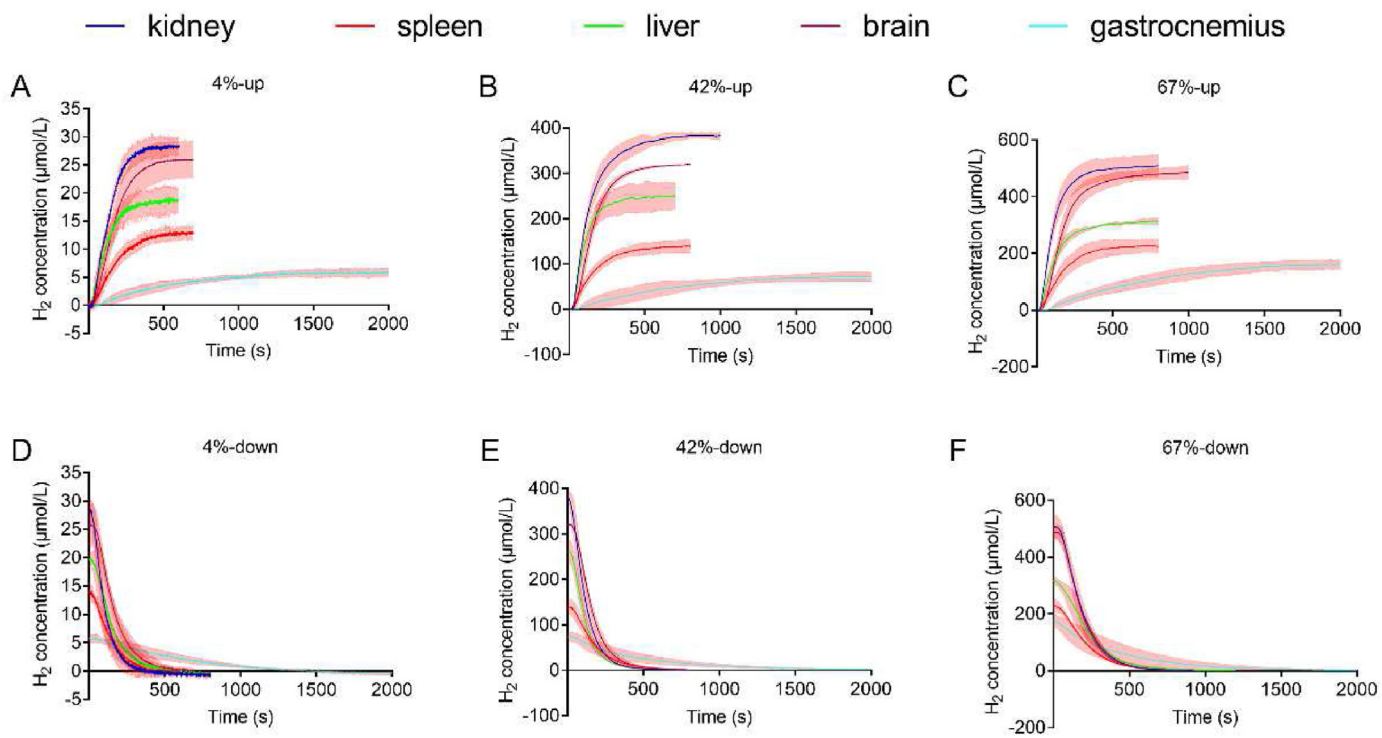

Figure 2. Real-time curve of H_2 concentration in the kidney, spleen, liver, brain, and gastrocnemius. (A–C) Changes of H_2 concentrations during inhaling different concentrations of H_2 (4%, 42% and 67%) (D–F) Changes of H_2 concentrations after ending inhaling different concentrations of H_2 (4%, 42% and 67%). Data are shown as the mean ± SD (n = 3–5 mice/tissue). The shaded areas around each line represents the 95% confidence interval.

of H_2 concentration varied in different tissues even after the same concentration of exogenous H_2 inhalation. Specifically, the H_2 concentrations in the kidney and brain rose at a faster rate, allowing both tissues to reach the saturated H_2 concentrations in a short time. The same ascent courses became slower in the liver and spleen. While the H_2 concentration in the gastrocnemius increased the slowest, and a long time was needed to reach a lower equilibrium concentration. When exogenous H_2 inhalation was stopped, the H_2 concentrations in the tissues began to decrease over time. Similarly, the gastrocnemius needed more time to reach the baseline reading compared with the other tissues (Figure 2D–F).

3.2. Saturation concentration of H_2 in different tissues

As shown in Figure 3, most of the H_2 saturation concentrations detected in various tissues were significantly different after the same concentration of H_2 inhalation. The H_2 saturation concentrations were highest in the kidney (28.058 ± 0.949 μmol/L, 382.183 ± 5.336 μmol/L, 508.522 ± 23.260 μmol/L after 4%, 42% and 67% inhalation, respectively; the same below), followed by the brain (25.981 ± 1.657 μmol/L, 319.162 ± 0.899 μmol/L, 485.425 ± 14.110 μmol/L), liver (18.430 ± 1.199 μmol/L, 230.091 ± 6.584 μmol/L, 313.850 ± 7.335 μmol/L), and spleen (12.992 ± 0.628 μmol/L, 139.429 ± 8.901 μmol/L,

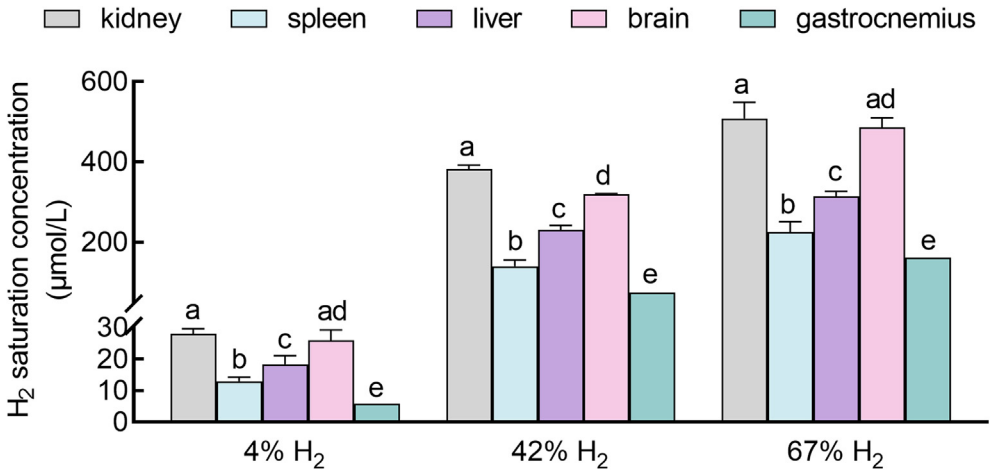

Figure 3. The saturation concentration of H_2 in the kidney, spleen, liver, brain, and gastrocnemius of mice after inhaling different concentrations of H_2 (4%, 42% and 67%). Data are shown as the mean ± SD (n = 3–5 mice/tissue). The statistical analysis was performed using one-way ANOVA followed by LSD test. Different letters indicate significant differences at $P < 0.05$ among tissues.

225.351 ± 14.711 μmol/L), and lowest in the gastrocnemius (5.927 ± 0.532 μmol/L, 73.364 ± 6.440 μmol/L, 160.765 ± 10.245 μmol/L). There was no significant difference of H_2 saturation concentration detected in the kidney and brain after the low and high concentrations of exogenous H_2 inhalation. Other inter-tissue comparisons all showed significant differences ($P < 0.05$). Attentively, the difference of H_2 saturation concentration detected in the same tissue was directly proportional to the difference of inhaled exogenous H_2 concentration, namely, the saturation values after inhaling 42% and 67% H_2 were about 12.3- and 17.8-time greater than that after 4% H_2 inhalation in various tissues except for the gastrocnemius with 67% (about 27.1-time).

4. Discussion

In this study, the real-time H_2 concentrations in five tissues of mice including brain, kidney, liver, spleen, and gastrocnemius were monitored after continuously inhaling three different concentrations of H_2 (4%, 42% and 67%) using the Unisense H_2 microsensor. Unsurprisingly, the results showed that H_2 concentration curves over time and H_2 saturation concentrations were significantly different among various tissues of mice (Figures 2 and 3), but similar with that in the corresponding tissues of rats except kidney and spleen (Figure 4).

Undoubtedly, the H_2 concentration is an important indicator for the quality evaluation of H_2 inhalation equipment and H_2-rich products. Currently, several methods including gas chromatography, H_2 microelectrode detection and redox titration (methylene blue) were often used to determine H_2 concentration.

Gas chromatography is a standard method for gas analysis, by which the concentration of H_2 in gas can be directly analyzed. However, H_2 dissolved in liquid (water or blood) must be released before measurement due to the interference of solvent signals. As early as 2007, Ohsawa determined H_2 concentration in blood using gas chromatography. They found that H_2 concentration in arterial blood increased after exogenous H_2 inhalation, and was higher than that in artery blood, which suggested that H_2 had been incorporated into tissues (Ohsawa et al., 2007). Other studies have also reported the H_2 concentrations in blood and/or tissues after exogenous H_2 treatment in rat models through this method (Nagata et al., 2009; Cardinal et al., 2010; Sobue et al., 2015). Liu et al. (2014) determined and compared the H_2 concentrations in various homogenized rat organs after several routes and doses of H_2 administration using high-quality sensor gas chromatography. They revealed different peak H_2 concentrations following one-time H_2 administration and the value changes over time (Liu et al., 2014). In one word, gas chromatography is popular for gas concentration determination, but this technique cannot realize real-time detection, and *in-vivo* studies are not yet possible.

The Unisense H_2 microsensor is a miniaturized Clark-type hydrogen sensor for measuring partial pressure of H_2. Driven by the external partial pressure, H_2 will pass through the sensor tip membrane and be oxidized at the platinum anode surface. The picoammeter converts the resulting oxidation current to a signal, and finally to H_2 concentration. Depending on its ultra-fine needle size tip, excellent response time, and high sensitivity, the H_2 sensor facilitates reliable and fast measurements, which makes it especially popular in some advanced applications such as long-term H_2 monitoring in tissues or water. In addition, the electrode analysis is relatively simple, given the data can be read directly in real time when

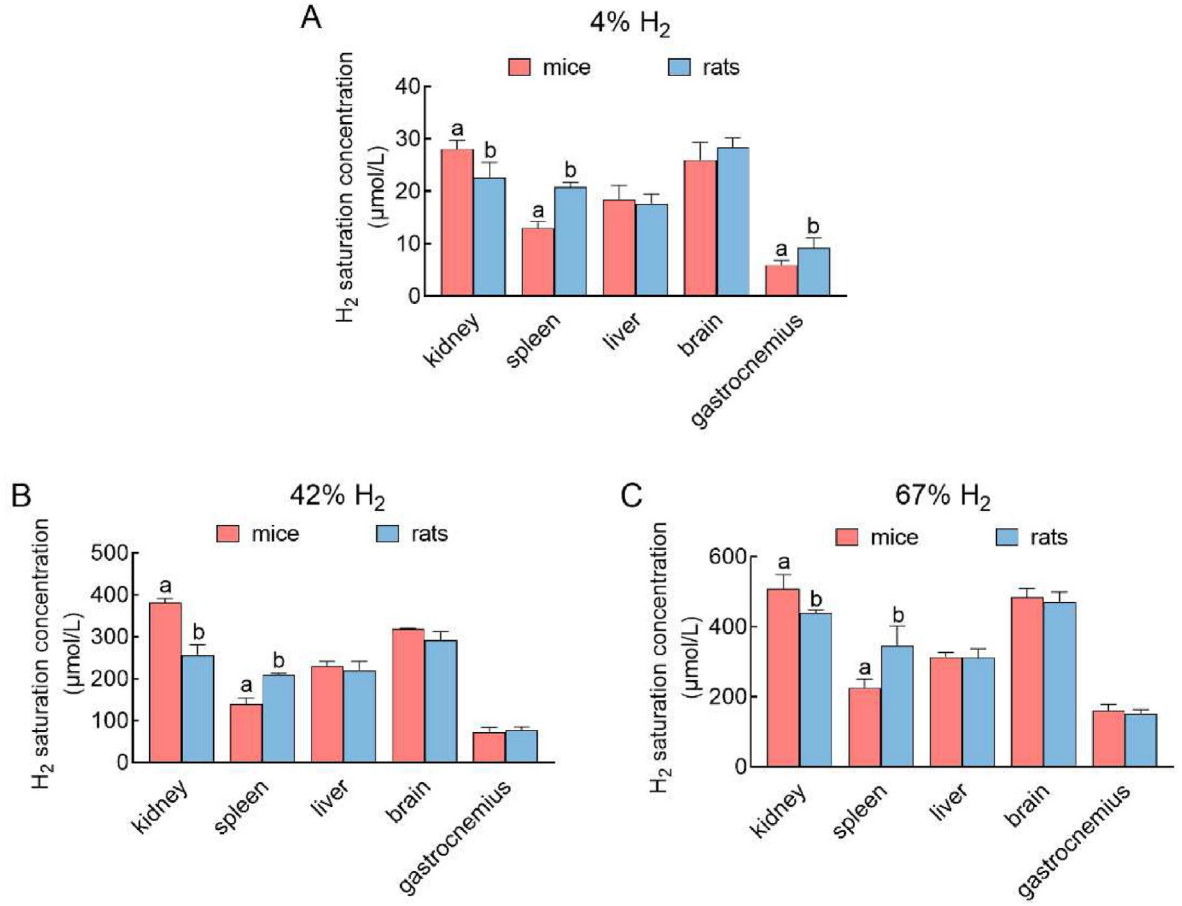

Figure 4. Comparison of the saturation concentration of H_2 in the kidney, spleen, liver, brain, and gastrocnemius of mice and rats after inhaling different concentrations of H_2 (4%, 42% and 67%). Data are shown as the mean ± SD (n = 3–5 mice/tissue). The statistical analysis was performed using the *independent samples t-test*. Different letters indicate significant differences of the saturation concentration of H_2 in the same tissue between the mice and rats ($P < 0.05$).

putting the electrode in H_2-containing water or target tissue. So, the microsensor is widely used in a series of studies to monitor the time-course of H_2 level changes in blood and tissues (Hayashida et al., 2008; Sobue et al., 2015; Yamamoto et al., 2019; Liu et al., 2022). During the measurement process, the mouse skin opening should be as small as possible. It can be considered to put a moist gauze on the exposed tissue, and the normal saline can also be sprayed intermittently to avoid tissue drying, so as to better simulate the *in vivo* environment and obtain more accurate measurement data. Nevertheless, the electrode measurement is not completely precise due to the interference of bioelectrical signals, which has become a bottleneck restricting the analysis of H_2 concentration *in vivo*.

Here, the dynamic distribution of H_2 in different tissues of another commonly used experimental rodent mice was explored after three different concentrations of exogenous H_2 Inhalation. The results showed that the concentration of H_2 in tissues depended on the time, the concentration of exogenous H_2 intake as well as the characteristics of the tissue itself. After the exogenous H_2 was inhaled by mice, it diffused through the alveoli into the bloodstream, then dissolved, and was transported through the whole body in a blood flow-dependent manner (Ichihara et al., 2021) despite of the unclear receptor molecules and downstream effectors (Sano et al., 2020). Instead of being concentrated in the blood vessels, H_2 diffused out of the blood vessels during travelling (Sano et al., 2020). It has been verified by the breath analysis that 60% was excreted in the breath and the rest was consumed by the body (Shimouchi et al., 2012, 2013). The dissolved or diffused H_2 entered tissues by a pressure gradient. In this study, the H_2 saturation concentration was highest in the kidney of mice, and followed by the brain, liver, spleen and lowest in the gastrocnemius (Figures 2 and 3).

As the organ with the most abundant blood supply of the whole body, kidneys receive approximately 20%–25% of the cardiac output (Povstyan et al., 2011). They are normally blooded from renal arteries that anatomically originates from the abdominal aorta (Karadağ et al., 2020). The dissolved H_2 was transported into the kidneys along with the bloodstream of systemic circulation. In view of the abundant blood supply of the kidneys, H_2 was saturated in a short time and the peak H_2 concentration was the highest under any concentration of H_2 inhalation. So H_2 in the kidneys was mainly transported in a blood flow-dependent manner after inhalation despite the gaseous diffusion could not be excluded. The results were not completely consistent with the reports of Yamamoto et al. (2019) and Liu et al. (2022), where the H_2 saturation concentration in the kidney was not higher than that in the brain and even more other organs (Yamamoto et al., 2019; Liu et al., 2022).

The H_2 saturation concentration in the brain is second to that in the kidney only. There were no significant differences detected in H_2 concentrations of the two tissues after inhaling low or high concentrations of H_2. The cerebral blood mainly comes from the carotid arterial, and its blood flow accounts for about 15% of the total cardiac output (Yu et al., 2016). As of now, several studies have explored the H_2 concentration in arterial blood after H_2 inhalation. Hayashida et al. (2008) investigated the regional delivery of inhaled 2% H_2 by monitoring the time-course of H_2 level changes in blood and myocardium by the aid of a needle-shaped H_2 sensor, and found that H_2 inhalation could efficiently increase the H_2 concentration in the arterial blood and "at risk" area of myocardial infarction and then alleviate ischemia-reperfusion injury (Hayashida et al., 2008). Sano et al. (2020) investigated the kinetics of single-dose inhalation of H_2 in the body of pigs. The results showed that H_2 concentration of carotid artery reached a very high level immediately after inhalation, indicating that the inhaled H_2 entered in the brain efficiently (Sano et al., 2020). Liu et al. (2014) reported that inhalation of H_2 induced slightly higher H_2 concentration in the brain compared to the other modes of H_2 administration (Liu et al., 2014). Yamamoto et al. (2019) showed that H_2 concentration would increase more rapidly and saturate at a higher value in the brain due to the short distance between the gas supply hood and the tissue, which was attributed to the gaseous diffusion model based on the fact that H_2 can traverse the blood–brain barrier (Yamamoto et al., 2019). Fortunately, the results of Yamamoto's study, our previous research in rats inhaling 4% H_2 (Liu et al., 2022), and the current study were similar. So, we inferred that both gas diffusion and bloodstream transport contributed to the H_2 concentration in the brain considerably after the H_2 inhalation.

Liver, the largest internal organ, has extremely rich blood flow. Moreover, the liver has strong ability to accumulate H_2 after exogenous supplement due to the high affinity of hepatic glycogen to hydrogen molecule (Kamimura et al., 2011). The previous study has detected the highest peak H_2 concentration in the liver of rats after inhaling 3% H_2 (Yamamoto et al., 2019). However, this study and our previous research have not detected such high H_2 concentration in the liver, which may result from the operational differences (Liu et al., 2022). The alleviating effects of H_2 on liver diseases are unquestionable, which has also been evidenced in our own investigation (Liu et al., 2020). As the largest immune organ, spleen can store part of blood in the sinuses. Here, the lowest H_2 concentration was detected in the spleen of the abdominal organs. We speculated that inhalation may not be a suitable way to ingest H_2 for the spleen, which has ever been shown in the study of Liu et al. (2014) (Liu et al., 2014). Consistent with most other studies, thigh muscle required a longer time to saturate and the H_2 saturation concentration was the lowest (Hayashida et al., 2008; Yamamoto et al., 2019; Liu et al., 2022). Following the blood flow model, H_2 concentration would increase more gradually in the muscle than other organs due to lower blood flow (Yamamoto et al., 2019; Liu et al., 2022).

H_2 concentration in arterial blood is proportional to the partial pressure of H_2 in the inhaled gas mixture (Sano et al., 2020). Similarly, a dose-dependent response of H_2 concentrations in the same tissue of mice after inhaling different concentrations of H_2 was found, which was consistent with the results in tissues of rats (Liu et al., 2022). By comparing the H_2 saturation concentrations in the same tissue after the same concentration of exogenous H_2 inhalation between rats and mice in detail, we found no differences of H_2 saturation concentrations in the liver and brain between both animals, regardless of any H_2 concentration inhaled. However, for the kidney and spleen, the results were reversed, with significant differences in H_2 concentrations detected in both tissues ($P < 0.05$). The H_2 saturation concentrations detected in gastrocnemius of mice and rats were significantly different after low concentration of H_2 inhalation, but there was no difference after medium and high concentrations of H_2 inhalation (Figure 4). The differences of the results reflected an inevitable problem during the measurement, the varieties among animals. After the same concentration of exogenous H_2 inhalation, the H_2 concentration detected in the same tissue of different mice may vary. For example, the H_2 concentration in the liver of mice ranged from about 12 to 22 μmol/L after 4% H_2 inhalation, and only five similar H_2 concentration curves were obtained in eight detected mice. The situation has close relationships to the physical differences of mice and the practical operation of measurement. Practical considerations include periodic calibration of the sensor with H_2 standards and the membrane permeability of the H_2 microsensor, which may decrease the sensitivity over time (Zhao et al., 2016).

Unfortunately, there are also some shortcomings in current research. Firstly, only inhalation was adopted here, whereas the distribution of H_2 in the body and the saturation concentrations of tissues may differ using other administration methods including drinking and injection. Secondly, detections of H_2 concentrations in the immediate target tissues such as respiratory and cardiovascular systems (including arterial and venous blood) were lacking, which were important to explore whether the H_2 concentration in the lung was the highest or not after inhalation, and to support the hypothesis that H_2 diffuses while being carried in a blood flow-dependent manner instead of diffusion simply (Sano et al., 2020). When the microsensor penetrated the lung, it might affect animals' normal breathing. And what was the worse, bleeding would be caused when the heart and blood vessels were penetrated, resulting in the change of blood volume, which might affect the blood flow and the amount of blood entering the tissue further. In addition, the spilled blood

could easily clog the sensor tip. Meanwhile, the contraction and expansion of the lung together with the constant beating of the heart could easily lead to the sensor tip bending or rupture. All the above conditions could interfere the accuracy of the measurement results. Based on the above statement, more advanced techniques and equipment were required to achieve precise *in vivo* measurement of gas concentration in tissues though H_2 sensing shows more promise as an effective means.

In conclusion, dynamics of H_2 concentrations over time in different tissues of mice exposed to continuous different concentrations of H_2 gas inhalation were investigated. Significantly various H_2 saturation concentrations among tissues were detected. The kidney and brain reached a higher H_2 saturation concentration while the gastrocnemius had the lowest and required a longer time to saturate. H_2 could reach to most organs not only by simply diffusion but also following transportation of the bloodstream. All the results provide a data reference for the dosage selection and the dose duration, and finally guarantee the optimal effects of H_2.

Declarations

Author contribution statement

Wenjun Zhu: Performed the experiments; Contributed reagents, materials, analysis tools or data.

Qianqian Gu: Performed the experiments; Analyzed and interpreted the data.

Boyan Liu: Conceived and designed the experiments; Performed the experiments.

Yanhong Si, Huirong Sun, Jingjie Zhong, Yi Lu, Dan Wang: Performed the experiments.

Junli Xue: Conceived and designed the experiments; Analyzed and interpreted the data; Wrote the paper.

Shucun Qin: Contributed reagents, materials, analysis tools or data; Wrote the paper.

Funding statement

Wenjun Zhu was supported by National Training Program for Undergraduate Innovation and Entrepreneurship [S202010439011].

Shucun Qin was supported by Academic promotion programme of Shandong First Medical University [2019QL010].

Data availability statement

Data will be made available on request.

Declaration of interest's statement

The authors declare no conflict of interest.

Additional information

No additional information is available for this paper.

References

Cardinal, J.S., Zhan, J., Wang, Y., Sugimoto, R., Tsung, A., McCurry, K.R., Billiar, T.R., Nakao, A., 2010. Oral hydrogen water prevents chronic allograft nephropathy in rats. Kidney Int. 77 (2), 101–109.

Cheng, J., Tang, C., Li, X., Hu, J., Lu, J., 2020. Hydrogen molecules can modulate enzymatic activity and structural properties of pepsin in vitro. Colloids Surf. B Biointerfaces 189, 110856.

Ge, L., Qi, J., Shao, B., Ruan, Z., Ren, Y., Sui, S., Wu, X., Sun, X., Liu, S., Li, S., Xu, C., Song, W., 2022. Microbial hydrogen economy alleviates colitis by reprogramming colonocyte metabolism and reinforcing intestinal barrier. Gut Microb. 14 (1).

Ge, L., Yang, M., Yang, N.N., Yin, X.X., Song, W.G., 2017. Molecular hydrogen: a preventive and therapeutic medical gas for various diseases. Oncotarget 8 (60), 102653–102673.

Guan, W.J., Wei, C.H., Chen, A.L., Sun, X.C., Guo, G.Y., Zou, X., Shi, J.D., Lai, P.Z., Zheng, Z.G., Zhong, N.S., 2020. Hydrogen/oxygen mixed gas inhalation improves disease severity and dyspnea in patients with Coronavirus disease 2019 in a recent multicenter, open-label clinical trial. J. Thorac. Dis. 12 (6), 3448–3452.

Hayashida, K., Sano, M., Ohsawa, I., Shinmura, K., Tamaki, K., Kimura, K., Endo, J., Katayama, T., Kawamura, A., Kohsaka, S., Makino, S., Ohta, S., Ogawa, S., Fukuda, K., 2008. Inhalation of hydrogen gas reduces infarct size in the rat model of myocardial ischemia-reperfusion injury. Biochem. Biophys. Res. Commun. 373 (1), 30–35.

Huang, P., Wei, S., Huang, W., Wu, P., Chen, S., Tao, A., Wang, H., Liang, Z., Chen, R., Yan, J., Zhang, Q., 2019. Hydrogen gas inhalation enhances alveolar macrophage phagocytosis in an ovalbumin-induced asthma model. Int. Immunopharm. 74, 105646.

Ichihara, G., Katsumata, Y., Moriyama, H., Kitakata, H., Hirai, A., Momoi, M., Ko, S., Shinya, Y., Kinouchi, K., Kobayashi, E., Sano, M., 2021. Pharmacokinetics of hydrogen after ingesting a hydrogen-rich solution: a study in pigs. Heliyon 7 (11), e08359.

Kamimura, N., Nishimaki, K., Ohsawa, I., Ohta, S., 2011. Molecular hydrogen improves obesity and diabetes by inducing hepatic FGF21 and stimulating energy metabolism in db/db mice. Obesity 19 (7), 1396–1403.

Karadağ, C., Birge, O., Bakir, M.S., Doğan, S., Tuncer, H.A., Şimşek, T., 2020. Encountering the accessory polar renal artery during retroperitoneal lymphadenectomy. Clin. Case Rep. 9 (1), 177–179.

Liu, B., Xie, Y., Chen, J., Xue, J., Zhang, X., Zhao, M., Jia, X., Wang, Y., Qin, S., 2021. Protective effect of molecular hydrogen following different routes of administration on D-galactose-induced aging mice. J. Inflamm. Res. 14, 5541–5550.

Liu, B., Xue, J., Zhang, M., Wang, M., Ma, T., Zhao, M., Gu, Q., Qin, S., 2020. Hydrogen inhalation alleviates nonalcoholic fatty liver disease in metabolic syndrome rats. Mol. Med. Rep. 22 (4), 2860–2868.

Liu, B.Y., Xue, J.L., Gu, Q.Q., Zhao, M., Zhang, M.Y., Wang, M.Y., Wang, Y., Qin, S.C., 2022. In vivo microelectrode monitoring of real-time hydrogen concentration in different tissues of rats after inhaling hydrogen gas. Med. Gas Res. 12 (3), 107–112.

Liu, C., Kurokawa, R., Fujino, M., Hirano, S., Sato, B., Li, X.K., 2014. Estimation of the hydrogen concentration in rat tissue using an airtight tube following the administration of hydrogen via various routes. Sci. Rep. 4, 5485.

Ma, X., Zhang, X., Xie, F., Zhao, P., Zhang, Z., Yi, Y., Zhang, X., Ma, S., Li, Q., Lv, B., Liu, M., Yao, M.A., Sun, X., Li, Y., 2020. Bio-enzyme basis of hydrogen in biological system. Curr. Biotechnol. 10 (1), 15–22.

Nagata, K., Nakashima-Kamimura, N., Mikami, T., Ohsawa, I., Ohta, S., 2009. Consumption of molecular hydrogen prevents the stress-induced impairments in hippocampus-dependent learning tasks during chronic physical restraint in mice. Neuropsychopharmacology 34 (2), 501–508.

Ohsawa, I., Ishikawa, M., Takahashi, K., Watanabe, M., Nishimaki, K., Yamagata, K., Katsura, K., Katayama, Y., Asoh, S., Ohta, S., 2007. Hydrogen acts as a therapeutic antioxidant by selectively reducing cytotoxic oxygen radicals. Nat. Med. 13 (6), 688–694.

Povstyan, O.V., Harhun, M.I., Gordienko, D.V., 2011. Ca^{2+} entry following P2X receptor activation induces IP_3 receptor-mediated Ca^{2+} release in myocytes from small renal arteries. Br. J. Pharmacol. 162 (7), 1618–1638.

Russell, G., Nenov, A., Kisher, H., Hancock, J.T., 2021. Molecular hydrogen as medicine: an assessment of administration methods. Hydro 2 (4), 444–460.

Sano, M., Ichihara, G., Katsumata, Y., Hiraide, T., Hirai, A., Momoi, M., Tamura, T., Ohata, S., Kobayashi, E., 2020. Pharmacokinetics of a single inhalation of hydrogen gas in pigs. PLoS One 15 (6), e0234626.

Shimouchi, A., Nose, K., Mizukami, T., Che, D.C., Shirai, M., 2013. Molecular hydrogen consumption in the human body during the inhalation of hydrogen gas. Adv. Exp. Med. Biol. 789, 315–321.

Shimouchi, A., Nose, K., Shirai, M., Kondo, T., 2012. Estimation of molecular hydrogen consumption in the human whole body after the ingestion of hydrogen-rich water. Adv. Exp. Med. Biol. 737, 245–250.

Sobue, S., Yamai, K., Ito, M., Ohno, K., Ito, M., Iwamoto, T., Qiao, S., Ohkuwa, T., Ichihara, M., 2015. Simultaneous oral and inhalational intake of molecular hydrogen additively suppresses signaling pathways in rodents. Mol. Cell. Biochem. 403 (1-2), 231–241.

Yamamoto, R., Homma, K., Suzuki, S., Sano, M., Sasaki, J., 2019. Hydrogen gas distribution in organs after inhalation: real-time monitoring of tissue hydrogen concentration in rat. Sci. Rep. 9 (1), 1255.

Yu, P., Wang, H., Mu, L., Ding, X., Ding, W., 2016. Effect of general anesthesia on serum β-amyloid protein and regional cerebral oxygen saturation of elderly patients after subtotal gastrectomy. Exp. Ther. Med. 12 (6), 3561–3566.

Zhao, D., Wang, T., Kuhlmann, J., Dong, Z., Chen, S., Joshi, M., Salunke, P., Shanov, V.N., Hong, D., Kumta, P.N., Heineman, W.R., 2016. *In vivo* monitoring the biodegradation of magnesium alloys with an electrochemical H_2 sensor. Acta Biomater. 36, 361–368.